Stepwise formation of a SMAD activity gradient during dorsal-ventral patterning of the *Drosophila* embryo

David J. Sutherland*, Mingfa Li, Xiao-qing Liu†, Raymund Stefancsik‡ and Laurel A. Raftery§

Cutaneous Biology Research Center, Massachusetts General Hospital/Harvard Medical School, Building 149, 13th Street, Charlestown, MA 02129, USA

*Present address: Department of Genetics, University of Cambridge, Cambridge CB2 3EH, UK
†Present address: Program in Genetics and Genomics, Hospital for Sick Children, Toronto, Ontario M5G 1X8, Canada
‡Present address: Veterinary Research Institute, Hungarian Academy of Sciences, Budapest H-1143, Hungary
§Author for correspondence (e-mail: laurel.raftery@cbrc2.mgh.harvard.edu)

Development 130, 5705-5716

doi:10.1242/dev.00801

Accepted 13 August 2003

Summary

Genetic evidence suggests that the *Drosophila* ectoderm is patterned by a spatial gradient of bone morphogenetic protein (BMP). Here we compare patterns of two related cellular responses, both signal-dependent phosphorylation of the BMP-regulated R-SMAD, MAD, and signal-dependent changes in levels and sub-cellular distribution of the co-SMAD Medea. Our data demonstrate that nuclear accumulation of the co-SMAD Medea requires a BMP signal during blastoderm and gastrula stages. During this period, nuclear co-SMAD responses occur in three distinct patterns. At the end of blastoderm, a broad dorsal domain of weak SMAD response is detected. During early gastrulation, this domain narrows to a thin stripe of strong SMAD response at the dorsal midline. SMAD response levels continue to rise in the dorsal midline region during gastrulation, and flanking plateaus of weak responses are detected in dorsolateral cells. Thus, the thresholds for gene expression responses are implicit in the levels of SMAD responses during gastrulation. Both BMP ligands, DPP and Screw, are required for nuclear co-SMAD responses during these stages. The BMP antagonist Short gastrulation (SOG) is required to elevate peak responses at the dorsal midline as well as to depress responses in dorsolateral cells. The midline SMAD response gradient can form in embryos with reduced *dpp* gene dosage, but the peak level is reduced. These data support a model in which weak BMP activity during blastoderm defines the boundary between ventral neurogenic ectoderm and dorsal ectoderm. Subsequently, BMP activity creates a step gradient of SMAD responses that patterns the amnioserosa and dorsomedial ectoderm.

Key words: BMP, Morphogen gradient, SMAD, Dorsal-ventral patterning, *Drosophila*

Introduction

Dorsal-ventral (DV) patterning of the *Drosophila* embryo is a paradigm for understanding the regulation of bone morphogenetic protein (BMP) activity. Some authors consider BMP-directed DV patterning to meet criteria for a morphogen gradient (e.g. Gurdon and Bourillot, 2001), but others point out that critical evidence is lacking (Neumann and Cohen, 1997). In this tissue, different levels of BMP activity can induce distinct cell fates (Ferguson and Anderson, 1992a), a defining feature for a morphogen (Slack, 1991). However, endogenous BMP protein has eluded detection in early embryos. Recently, an alternative method has been used to detect BMP activity, immunodetection of an activated signal transduction protein, phosphorylated-MAD (Dorfman and Shilo, 2001; Ross et al., 2001; Rushlow et al., 2001). These studies suggest that BMP activity does not form a continuous spatial gradient, as deduced from genetic analyses. This discrepancy led one group to question the BMP gradient model, and to propose that BMPs direct sequential binary cell fate choices during dorsal ectoderm patterning (Dorfman and Shilo, 2001). Here we demonstrate that patterns of BMP activity change, and induce a step gradient of responses at the onset of gastrulation.

BMP signaling is complex in early embryos, requiring two BMP ligands, Screw (SCW) and Decapentaplegic (DPP), and two type I receptor serine-threonine kinases, Saxophone (SAX) and Thickveins (TKV) (reviewed by Raftery and Sutherland, 1999). Receptors and SMAD signal transducers are present in the oocyte, so that the onset of signaling depends on zygotic transcription of ligand genes. *dpp* is expressed over the dorsal 40% of the embryo during blastoderm and gastrula stages (St. Johnston and Gelbart, 1987), whereas *scw* is expressed globally for a short period during blastoderm cellularization (Arora et al., 1994).

Patterns of ligand RNA accumulation are broader than the BMP activity gradient inferred from the pattern of dorsal fates (reviewed by Podos and Ferguson, 1999). A narrow band of dorsal midline cells become amnioserosa, the dorsal-most fate, in response to high BMP activity (Ferguson and Anderson, 1992a; Wharton et al., 1993). Both ligands, DPP and SCW, are required for this fate (Arora et al., 1994; Neul and Ferguson, 1998; Nguyen et al., 1998). In *scw* null or weak *dpp* mutants, the DV fate map shifts, so that amnioserosa is lost, the dorsal ectoderm contracts, and ventral ectoderm expands. In *dpp* null mutants, all ectoderm adopts the ventral ectoderm fate.

The domain of BMP activity is narrowed through antagonism by Short gastrulation (SOG), in collaboration with

other proteins (reviewed by Harland, 2001; Ray and Wharton, 2001). SOG is a secreted BMP binding protein, which is distributed in the inverse pattern to the proposed BMP activity gradient (Srinivasan et al., 2002). Consistent with a role for SOG as a BMP antagonist, *sog* null embryos have an expanded dorsal ectoderm (Ferguson and Anderson, 1992b; Francois et al., 1994). Surprisingly, *sog* null embryos lack the expansion of amnioserosa predicted for a BMP antagonist. Instead, they differentiate only a few amnioserosa cells. Genetic manipulations consistently support a positive role for SOG in amnioserosa patterning (Ashe and Levine, 1999; Decotto and Ferguson, 2001). This dual role led to a proposal that SOG directs ligand transport from lateral to dorsal regions (Holley et al., 1996), a model that has received recent experimental support (Eldar et al., 2002; Ross et al., 2001).

The BMP activity gradient was interpreted from the patterns of BMP-directed gene expression and terminally differentiated cell types. BMP target genes are expressed in domains centered on the dorsal midline, with smaller expression domains nested within the larger ones (Ashe et al., 2000; Jazwinska et al., 1999). However, the pattern of target gene expression also depends on Brinker, a transcriptional repressor that competes with BMP-activated SMADs to regulate target genes (Ashe et al., 2000; Jazwinska et al., 1999). After blastoderm, BMP activity negatively regulates *brinker*, limiting expression to the ventral ectoderm domain. In addition, BMP activity positively regulates genes that elevate BMP activity, including *dpp* (Biehs et al., 1996; Zhang et al., 2001). Thus, BMP-dependent gene expression is a complex output of direct and indirect responses. Assays to detect direct BMP responses are essential to understand the mechanisms for spatial deployment of active BMPs.

SMAD proteins mediate the gene expression responses to TGFβ superfamily ligands (reviewed by Massague and Wotton, 2000; Raftery and Sutherland, 1999). Two classes of SMADs collaborate to transduce the intracellular signal from the transmembrane receptor complex to the nucleus, the receptor-regulated SMADs (R-SMADs) and the common-mediator SMADs (co-SMADs). For *Drosophila* BMP signaling, MAD is the key R-SMAD and Medea is the only co-SMAD. MAD is directly phosphorylated in response to BMP signaling. Phospho-MAD (P-MAD) accumulates in the nucleus, associates with other transcription factors and binds DNA. Like the vertebrate co-SMAD, SMAD4, Medea accumulates in nuclei of cultured cells only in the presence of a phosphorylated R-SMAD. Co-SMADs also bind DNA and participate in transcription regulatory complexes. Detection of signal-dependent SMAD responses, whether as nuclear accumulation or phosphorylation, visualizes the pattern of active responses to TGFβ family signals. Here we find that patterns of co-SMAD responses undergo two transitions during blastoderm and gastrula stages, to form a step gradient of domains with different response levels. Formation of the step gradient requires both BMP ligands and SOG. The evolving pattern of BMP responses provides important insights into BMP-directed patterning of dorsal fates.

Materials and methods

Fly strains and genetic manipulations

Alleles and transgenes are described in FlyBase. Flies were reared on cornmeal-agar-glucose medium; embryos were collected on molasses plates. Embryo staging is according to Campos-Ortega and Hartenstein (Campos-Ortega and Hartenstein, 1985). The following strains were used:

$y^1\ w^{67c53}$ for wild type (WT)

dpp^{H46} *Sp cn bw/CyO23,* $P\{dpp^{Sal20}ry^{+t7.2}$*=dpp-sal20}* ($dppH^+$) (Wharton et al., 1993)

b scw^{12} *pr/CyO,* $P\{ry^{+t7.2}$*=ftz/lacZ}*

y sog^{Y506}*/FM7a*

sog^{U2}*/FM7a*

Dp(2;2)DTD48, $dpp^{d\text{-}ho}$ (4X*dpp*)

P{Ubi-p63E-Med.D} (*ubi>Medea*) (Das et al., 1998).

To express activated receptors in early embryos, *w; P{w+mC=GAL4-nos.NGT}* females (*nos>Gal4*) (Barrett et al., 1997) were mated to males of $P\{mw^+$*=uas-tkvA}/CyO* or $P\{mw^+$*=uas-saxA}* on III (Haerry et al., 1998).

To overexpress Medea we used either homozygous *Ubi>Medea* or *P{GAL4-prd.F}* (*prd>Gal4*) (Brand and Perrimon, 1993) driving *UAS>Medea*.

For larval protein extracts, *red mwh e* Med^1*/Df(3R)KpnA, ca awd* or Mad^{10} *b pr/*Mad^{12} *b pr* wandering third instar larvae were selected by their transparency.

For ventro-lateralized embryos, homozygous $cact^{PD74}$ *cn bw* females were obtained at 18°C and mated to $y^1\ w^{67c53}$ males at 25°C.

Germline clones were generated using the FLP-DFS system as described (Chou and Perrimon, 1996). For *Medea*, we generated clones in either $P\{ry^{+t7.2}$*=neoFRT}82B* Med^{13} (Hudson et al., 1998) or $P\{ry^{+t7.2}$*=neoFRT}82B* Med^8 (Wisotzkey et al., 1998) females, which were mated to Med^{13}*/TM3* or Med^8*/TM3* males, respectively. *Mad* germline clones were generated in $P\{ry^{+t7.2}$*=hsFLP}12,* $y^1\ w^*$*;* Mad^{10} $P\{ry^{+t7.2}$*=neoFRT}40A* females, which were mated to Mad^{12}*/CyO* males. There have been conflicting reports on the fertility of females bearing germline clones homozygous for Mad^{12} (Das et al., 1998; Wisotzkey et al., 1998). We tested the two previously used heat-shock protocols on the two previously described *FRT* Mad^{12} strains; in each case, no embryos were obtained with this allele. The cause for differing results remains unknown.

Constructs

Medea constructs used the cDNA AF027729 (Wisotzkey et al., 1998). Two were generated by PCR: pET28MedFL contains codons 56-782 (stop) cloned into the *Sac*I site of pET28a (Novagen). pGEX5MedC1 contains codons 399-782 (stop) in frame with the GST open reading frame (ORF) in pGEX5X-1 (Pharmacia).

UAS>Medea: An *Eco*RI-*Xba*I fragment containing 3′ sequences from the cDNA in pBluescript was subcloned into the *Eco*RI-*Xho*I sites of pUAST (Brand and Perrimon, 1993), using T4 DNA polymerase to blunt the *Xho*I and *Xba*I ends. The 5′*Eco*RI fragment of the cDNA was sub-cloned into the resultant plasmid and sequenced. Transgenic flies were generated by the CBRC Transgenic Fly Core.

Anti-Medea antiserum

Full-length Medea fusion protein was expressed from pET28MedFL as recommended (Novagen). Bacterial extracts were subjected to SDS PAGE; fusion protein was excised and electro-eluted. Rabbit antiserum was produced at Poconos Rabbit Farm and Research Laboratory (Canadensis, PA).

Affinity purification followed established protocols (Harlow and Lane, 1988), using C-terminal fusion protein from pGEX5MedC1.

Immunohistochemistry

For most experiments, embryos were collected for 1 hour at 25°C, aged for 2 hours 50 minutes at 25°C, prepared and fixed as described (Wisotzkey et al., 1998). Unpurified antiserum was pre-adsorbed at 1/1000 in PBSS (PBS pH 7.4 containing 0.1% saponin and 3% normal goat serum) against WT embryos collected for 1 hour and aged for 1 hour 50 minutes at 25°C. Immunofluorescence experiments gave the

same results with either affinity-purified antiserum or pre-adsorbed antiserum. We used pre-adsorbed anti-Medea antiserum for most experiments. Primary and secondary antibodies were incubated with embryos in PBSS overnight. Pre-adsorbed anti-Medea antiserum was used at 1/1000. Anti-phospho-SMAD1 (PS1) (Persson et al., 1998) was used at 1/100. Prior to mounting in Vectashield (Vector Labs), embryos were incubated with 0.2 μM ToPro3 (Molecular Probes) in PBSS, and washed briefly. Images were collected on a Leica confocal microscope at a fixed gain for each experiment. Gain-matched WT and mutant images were paired and manipulated together in Adobe Photoshop.

Protein extracts and Western blotting

Embryos were dechorionated and homogenized in lysis buffer (PBS; 5% glycerol; 0.1% Triton X-100) with protease inhibitors (Roche). Lysates were centrifuged at 14,000 ***g*** for 10 minutes; supernatant was stored at –80°C. Wandering third instar larvae were homogenized for 20 minutes on ice, then centrifuged for 30 minutes at 14,000 ***g***. Western blots were performed as described (Li et al., 1999) with affinity-purified anti-Medea and chemiluminescence (Tropix). Blots were stripped (0.2 M glycine, 0.1% SDS, 1% Tween-20, pH 2.2) and re-probed with either monoclonal anti-actin (Chemicon International) or monoclonal anti-tubulin (Cedarlane Laboratories).

Results

A specific antiserum detects endogenous Medea

To develop an important tool, we generated rabbit polyclonal antiserum against recombinant Medea protein. Specificity for immunofluorescence was assessed using *Med*^{13}, a molecular null allele (Xu et al., 1998). Females bearing *Med*^{13} germline clones were mated to heterozygous males. Resultant embryos either lacked staining entirely or had a dorsal band of cells with variable nuclear staining (Fig. 1A), the zygotic null and heterozygous classes, respectively. Thus, pre-adsorbed antiserum was specific for immunofluorescence.

In protein extracts from WT or *Mad* mutant larvae, the antiserum strongly detected several polypeptides that were missing from *Medea* mutant larvae (Fig. 1B). The largest had an apparent molecular weight of approximately 97 kDa. This polypeptide has a slower mobility than predicted from the largest cDNA ORF (Das et al., 1998; Hudson et al., 1998; Wisotzkey et al., 1998; Xu et al., 1998). Polypeptides of similar mobility were produced from pCMBV5-HA-MEDEA (Wisotzkey et al., 1998) in 293MEK cells and *ubi>Medea* in flies (data not shown). The 97 kDa polypeptide was the predominant band detected in embryonic extracts (Fig. 1C,D).

Nuclear co-SMAD is BMP-dependent in early embryos

Endogenous BMP signals stimulate only a fraction of cytoplasmic MAD to accumulate in the nucleus (Dobens et al., 2000; Newfeld et al., 1997). In contrast, nuclear accumulation of endogenous Medea was detected in WT embryos (Fig. 1A, Fig. 2B,C). We investigated whether this was a response to TGFβ superfamily signals.

To determine whether BMP activity is necessary for nuclear Medea, we examined embryos with reduced BMP R-SMAD. There was no detectable nuclear accumulation of Medea and no stripe of increased staining in appropriately staged *Mad*^{10}/*Mad*^{12} embryos from *Mad*^{10} germline clones (Fig. 3G) (see Materials and methods). Consistent with the requirement for MAD, germline clones for C-terminally truncated Medea, which does not stably associate with MAD (*Med*^{8}) (Wisotzkey et al., 1998), yielded a defective class of embryos that lacked nuclear staining (data not shown). To test the effect of globally activated BMP signaling, we expressed the constitutively active BMP type I receptor TKVA (Haerry et al., 1998) using maternally provided GAL4 (*nos>Gal4*). The resultant embryos

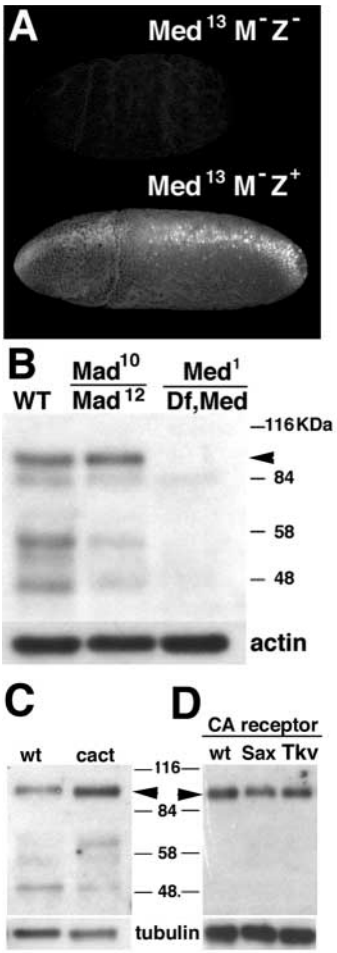

Fig. 1. Anti-Medea antiserum is specific. (A) Anti-Medea detected two classes of embryos from a mating of females bearing germline clones of the null allele *Med*^{13} with *Med*^{13}–/+ males. One class, zygotic heterozygotes (M^-Z^+), showed variable subcellular localization of the antigen, cytoplasmic in ventral and lateral regions, and nuclear in many dorsal cells. The other class lacked detectable staining, the zygotic null homozygotes (M^-Z^-). (B) Western analysis of larval extracts with affinity-purified anti-Medea antiserum, and actin as a control. Wild-type larvae (WT) and *Mad* mutant larvae (*Mad*^{10}/*Mad*^{12}) give a similar pattern of strongly staining bands of approximately 97 kDa (arrowhead in B-D), 55 kDa and 47 kDa. These bands were missing in protein extracts from *Medea* mutant larvae (*Med*^{1}/*Df Med*). (C,D) Comparison of steady state Medea levels in embryo extracts using Western blot analysis, with tubulin as a control. (C) WT versus embryos from *cactus*^{PD74} mothers (cact), to assess the contribution of dorsal tissues to total Medea levels. Total Medea is not decreased when dorsal tissues are absent. (D) WT versus globally increased BMP signaling through either constitutively active (CA) receptor, Sax (*nos>Gal4;UAS>saxA*) or Tkv (*nos>Gal4; UAS>tkvA).* Steady state Medea levels are unperturbed by hyperactivation of either BMP receptor.

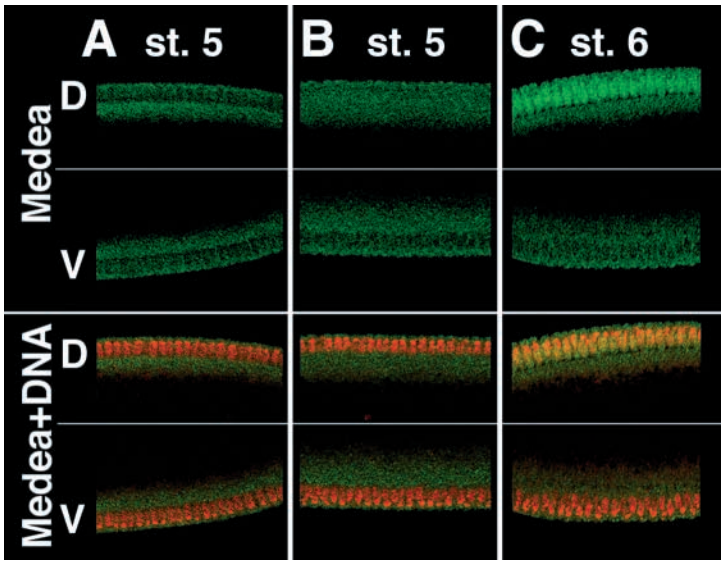

Fig. 2. Levels of Medea in dorsal nuclei increase sharply at the onset of gastrulation. Optical sections of wild-type (WT) embryos co-stained for Medea (green) and with the DNA dye ToPro3 (red). Dorsal (D) and ventral (V) midline cells from a single embryo are shown as paired images for each stage, with Medea staining alone (top pair) and merged with DNA dye (bottom pair). (A) Most stage 5 embryos have a subcellular distribution of Medea that is indistinguishable between dorsal and ventral cells, but a few (B) show uniform distribution of Medea between the nuclei and cytoplasm within a broad domain of dorsal cells. (C) At the onset of gastrulation, all embryos show strong nuclear accumulation of Medea within a narrow stripe of cells at the dorsal midline.

had strong nuclear accumulation of Medea throughout, beginning during cellularization (Fig. 3H). Thus, BMP signaling is both necessary and sufficient for nuclear accumulation of Medea in early embryos.

In WT embryos, Medea staining in dorsal midline cells was strikingly more intense than in other cells (Fig. 3A,C,E). This difference is not because of a difference in gene expression, for *Medea* transcripts accumulate uniformly throughout the early embryo (Wisotzkey et al., 1998). Alternatively, the intense Medea staining in dorsal midline cells could arise from higher protein levels in cells stimulated by BMP. We found no such effect in Western analysis. Embryos from homozygous *cactus*^{PD74} females had little or no PMAD staining (data not shown) because of loss of dorsal tissues (Roth et al., 1991), but no decrease in steady-state Medea levels compared with a tubulin control (Fig. 1C). Conversely, increased BMP activity gave no increase (Fig. 1D) in embryos with global expression of either constitutively active BMP type I receptor, TKVA or SAXA (Haerry et al., 1998). Thus, the strong staining in dorsal midline cells was not because of a signal-dependent increase in Medea protein levels. Instead, immunostaining is more sensitive to Medea in the nucleus than in the cytoplasm, making it a sensitive assay for levels of BMP activity.

Patterns of SMAD responses are dynamic

In most blastoderm embryos, levels of nuclear Medea were indistinguishable between dorsal and ventral cells (Fig. 2A). The earliest embryos in which dorsal cells had increased nuclear accumulation of Medea were late in stage 5, between the end of cellularization and the beginning of gastrulation (Fig. 2B). At this stage, nuclear accumulation was detected in a 32 cell-wide domain centered at the dorsal midline. Within this domain, nuclear staining appeared consistent over approximately 24 cells. At the edges, levels of nuclear Medea decreased over approximately four cells. More laterally, the level of nuclear staining was indistinguishable from that in ventral midline cells. Not all stage 5 embryos had significant nuclear Medea, suggesting that this phase is brief.

In contrast, early gastrula embryos had a narrow stripe

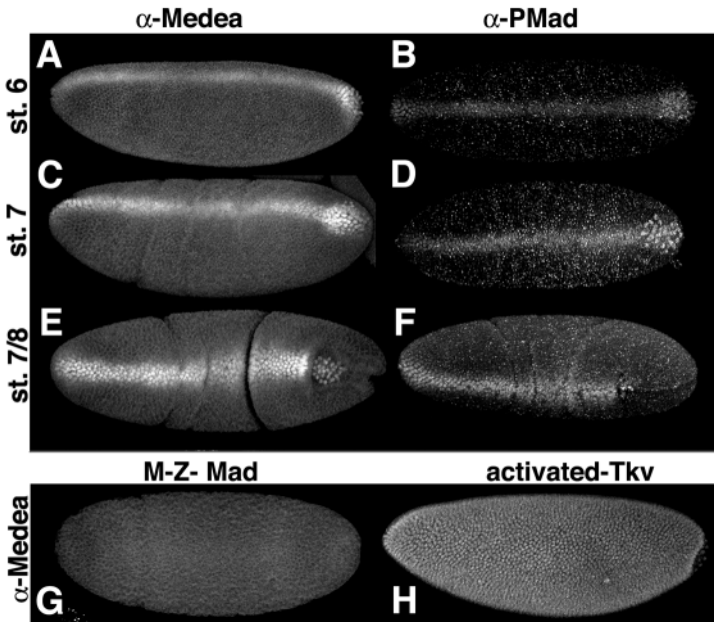

Fig. 3. Dorsal-midline stripe of SMAD responses expands and intensifies during early gastrulation. (A-F) Confocal projections of wild-type (WT) embryos stained for Medea (A,C,E), or PMAD (B,D,F). (B-G) Dorsal views or slightly rotated. (A,H) Side views, or slightly rotated. (A,B) Strong nuclear SMAD accumulation was co-incident with initial cellular changes in the cephalic furrow. (C-F) Levels of nuclear staining for both antigens intensified during gastrulation and early germband extension, and the midline stripe widened. (E,F) Response levels dropped dramatically over 2-3 cells at the edges of the stripe. (G) Medea nuclear localization was lost in an embryo lacking WT *Mad* (M-Z-Mad), and induced globally in embryos expressing constitutively activated TKV under the control of *nos>Gal4* (H). Note that somatic cells stain more intensely than posterior germ cell primordia, and that this embryo is at stage 5. Anterior is leftwards.

of approximately 5-7 cells with detectable nuclear Medea. Within this stripe, the central three cells had intense nuclear staining (Fig. 2C, Fig. 3A); nuclear staining dropped sharply across two cells at each edge. Thus, the domain of detectable co-SMAD response narrowed significantly, as levels increased at the dorsal midline.

In our experiments, the earliest PMAD staining was detected at the beginning of gastrulation, co-incident with the narrow stripe of strong Medea staining (Fig. 3B,D). More sensitive assays detected an earlier broad domain of weak PMAD staining during cellularization (Ross et al., 2001; Rushlow et al., 2001), similar to the earliest nuclear Medea pattern. For PMAD, the broad domain of weak response was detected during mid-cellularization, and the transition to a narrow stripe of strong response was detected during late cellularization (Rushlow et al., 2001), in both cases earlier than for Medea. Technical differences between antibodies and staining techniques may contribute to this difference. It may also reflect the time between receptor activation at the cell surface and SMAD accumulation in the nucleus, which takes 15-20 minutes for activin responses in *Xenopus* cells (Bourillot et al., 2002). Stage 5 cellularization spans 40 minutes (Campos-Ortega and Hartenstein, 1997).

SMAD-response patterns changed further during gastrulation (stages 6-7), a period of approximately 20 minutes. For both nuclear Medea and PMAD, the domain of most intense staining widened to include approximately 7-9 cells (Fig. 3E,F, Fig. 4). In the midline stripe, nuclear Medea staining intensified, but maintained a sharp decline at each edge. The stripe pattern persisted in the cephalic region (Fig. 4A). Between the cephalic furrow and the posterior furrow, the domain of intense staining became irregular, as presumptive amnioserosa cells rearrange to accommodate the extending germband (reviewed by Campos-Ortega and Hartenstein, 1997). During mid- to late-gastrulation, dorsolateral domains with low nuclear Medea were detected, which encompassed approximately 6-7 cells beyond the intensely staining region (Fig. 4). These cells had a uniform distribution of Medea that was distinct from the nuclear staining in more dorsal cells (compare Fig. 4D,D' with Fig. 4B,B'). More ventral cells showed staining in the cytoplasm, with occasional speckles staining the nuclei (Fig. 4C,C'). The speckles may reflect shuttling through the nucleus in the absence of TGFβ family signals (Pierreux et al., 2000).

The stage 7 step gradient observed for Medea nuclear responses may involve the same cells as the stage 5/6 step gradient reported for PMAD (Rushlow et al., 2001). The two stages cannot be directly compared because of cell movements during germband extension. Alternatively, the cells with weak PMAD responses at stage 5 may show strong nuclear localization of Medea by stage 7. The shoulders of weak PMad staining at stage 5 encompass the expression domain for *u-shaped* (Rushlow et al., 2001), which extends into the presumptive dorsomedial ectoderm (Ashe et al., 2000). The shoulders of weak Medea responses also extend into the presumptive dorsal ectoderm, and encompass the *u-shaped* expression domain at stage 7/8 (Berkeley Drosophila Genome Project, Expression Patterns, http://www.fruitfly.org/cgi-bin/wx/insitu.pl).

In summary, Medea responses to BMP activity form three distinct patterns, beginning with a weak dorsal response at cellular blastoderm. At the onset of gastrulation, the pattern narrows to a strong dorsal midline response. The midline response intensifies and spreads during gastrulation, when flanking dorsolateral domains develop weak Medea responses. This step gradient of responses does not include as many lateral cells as the initial blastoderm response.

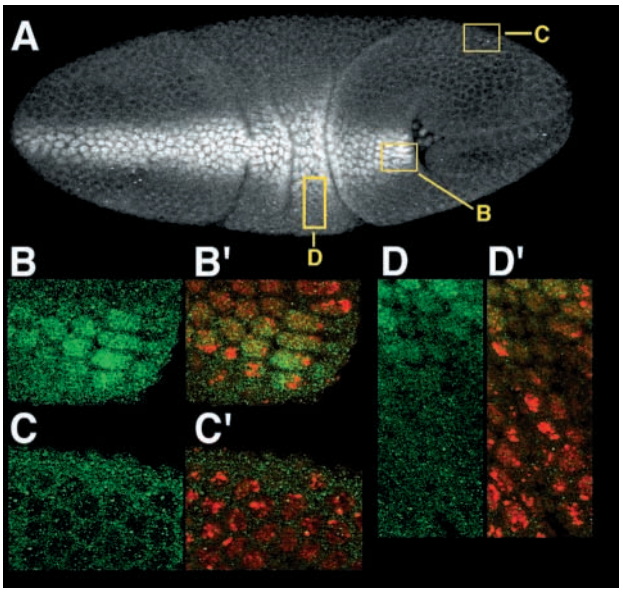

Fig. 4. Low nuclear Medea accumulates in dorsolateral cells during late gastrulation. (A) Confocal projection of Medea staining in a stage 8 embryo, with regions of high magnification, single optical sections (B-D) indicated with yellow boxes. Medea immunofluorescence in white (A) or green (B, B',C,C',D,D') and Topro3 DNA stain in red (B',C' and D'). Nuclei stained with Topro3 are diffuse red with bright spots of condensed chromatin. (A). At the midline, nuclei have higher levels of Medea than the cytoplasm (B,B'). Medea is largely excluded from nuclei in ventral ectoderm cells (C,C'; dorsal here because of germband extension). In dorsolateral cells there is an even distribution of Medea between the cytoplasm and the nucleus. This shoulder of low signal is absent anterior to the cephalic furrow. B-D were collected at the same gain. Anterior is leftwards.

Sharp transitions in BMP activity correlate with pattern boundaries

To test the correlation between the domain of intense SMAD responses and the position of dorsal pattern markers, we examined the cell division 14 mitotic domains 1, 3 and 5 of the cephalic region (Arora and Nüsslein-Volhard, 1992). Mitotic domains are spatially restricted regions of cells that undergo synchronous mitosis after cellular blastoderm (Foe et al., 1993). Condensed mitotic chromosomes were detected with ToPro3 DNA dye in embryos stained for Medea or PMAD. Mitotic domain 3 precisely straddled the stripe of peak SMAD response; the dorsolateral domains 1 and 5 abutted its edges (Fig. 5A,B). Mitotic domains 3 and 5 remained abutted to the narrower midline response in 1X*dpp* embryos (Fig. 5C) and also to the wider midline response in *4Xdpp* embryos (Fig. 5D-PMAD, and data not shown-Medea). A broader domain 3 straddled the broader SMAD response stripe of *4Xdpp* embryos. Thus, the edges of the midline stripe define

transitions between BMP activity levels that direct different cell fates.

The dorsolateral co-SMAD response requires both ligands

The spatial gradient model (reviewed by Podos and Ferguson, 1999) and the sequential patterning model (Dorfman and Shilo, 2001) predict different roles for SCW in dorsal ectoderm patterning, as well as different timing for patterning this fate.

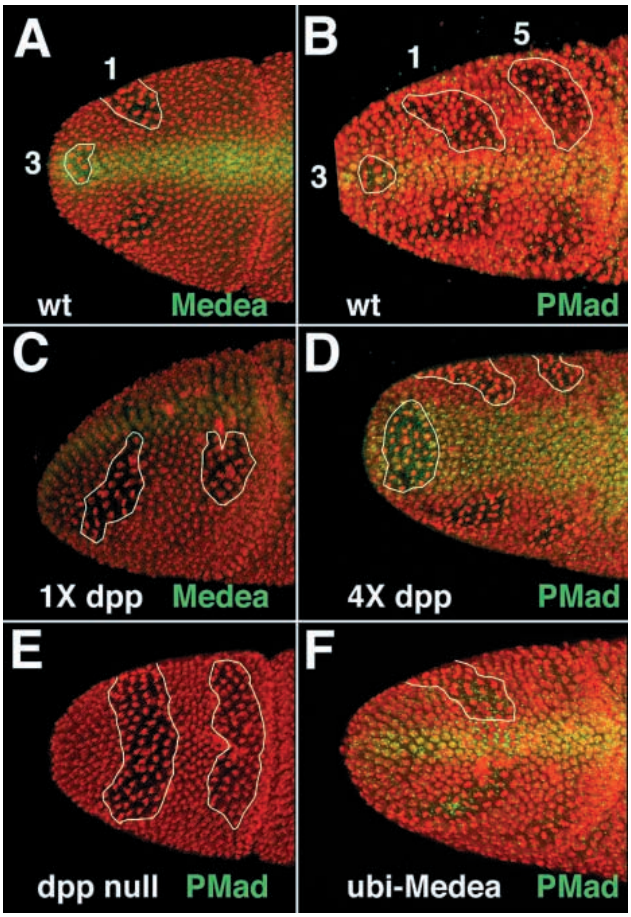

Fig. 5. Division 14 mitotic domains are positioned relative to threshold levels of SMAD responses. Cephalic regions of embryos stained for Medea (A,C) or PMAD (B,D,E,F) (both green), and ToPro3 (red), dorsal views except C. ToPro3 DNA dye intensely stains highly condensed mitotic chromosomes. One of each paired domain is outlined in white. (A,B) The dorsal edges of mitotic domains $\delta_{14}1$ (1) and $\delta_{14}5$ (5) abut the lateral edges of the midline stripe of high-level SMAD response, either nuclear Medea (A) or PMAD (B). Mitotic domain $\delta_{14}3$ (3) has the same width as the stripe. (C-E) These domains retain their position relative to the altered stripe in embryos with altered *dpp* gene dosage. (C) Domains $\delta_{14}1$ and $\delta_{14}5$ still abut the narrow, weak Medea stripe in dpp^{H46}/+ embryos (*1Xdpp*). (D) Each pair of domains $\delta_{14}1$ and $\delta_{14}5$ is wider apart, but each domain still abuts the broad PMAD stripe in *Dp(2;2)DTD48/Dp(2;2)DTD48* embryos (*4Xdpp*). Domain $\delta_{14}3$ fully spans the broader stripe. (E) Domains $\delta_{14}1$ and $\delta_{14}5$ fuse at the midline in dpp^{H46}/dpp^{H46} embryos (*dpp* null), PMAD staining and $\delta_{14}3$ are lost. (F) PMAD staining is more intense in embryos expressing high levels of Medea from a transgene (*ubi>Medea*), but the mitotic domains still abut the stripe. Anterior is leftwards.

We wished to determine the relative contributions of DPP and SCW to the SMAD response patterns.

To investigate the role of DPP, we stained embryos produced by dpp^{H46}*/CyO23, P{*dpp^{H+}*}* adults. Within the resultant population of stage 6 embryos, some lacked nuclear Medea (Fig. 6A). Similarly, PMAD staining was absent in some embryos; occasional staining in primordial germ cells of such embryos may be artifactual (Fig. 6B). Late-gastrula *dpp* mutants were visibly distinct, and lacked SMAD responses (Fig. 5E). Thus, DPP is necessary for both SMAD responses.

To determine the role of SCW, we stained embryos produced from scw^{S12}*/CyO, ftz-lacZ* adults, so that *scw* embryos were identified by absence of β-galactosidase. Consistent with a previous report (Dorfman and Shilo, 2001), PMAD staining was at background levels in somatic tissues of *scw* embryos (Fig. 6D). Similarly, Medea was not detected in dorsal nuclei of *scw* embryos at this stage, although some *scw* embryos showed a subtle increase in Medea staining in the apical cytoplasm (Fig. 6C and data not shown). Even at stage 7, when dorsolateral nuclei of WT embryos accumulate low levels of Medea, it was undetectable in dorsal-most nuclei of *scw* embryos. Although the dorsal-most cells of *scw* embryos adopt a dorsal ectoderm fate, these cells do not exhibit the weak nuclear Medea response that arises in dorsolateral cells of WT embryos. Thus, both DPP and SCW are necessary for both the strong midline and weak dorsolateral domains of SMAD responses during gastrulation, consistent with the gradient model.

The level of peak response is sensitive to *dpp* dosage

DV patterning is highly sensitive to DPP levels. Loss of one copy of *dpp* is lethal, causing a range of defects in head skeleton and amnioserosa patterning (Irish and Gelbart, 1987; Wharton et al., 1993). Increased *dpp* dosage leads to more amnioserosa cells (Wharton et al., 1993). Thus, we investigated the effects of *dpp* dosage on the patterns of SMAD responses. Contrary to a previous report (Dorfman and Shilo, 2001), we found a variable dorsal midline response in most *dpp*-/+ embryos.

For this experiment, we examined both PMAD and Medea staining in embryos from a mating of dpp^{H46}*/P{*dpp^{H+}*}* with WT. Resultant embryos were either dpp^{H46}/+ (1X*dpp*) or *P{*dpp^{H+}*}* plus the two endogenous copies of the gene (3X*dpp)*. Wild-type embryos were stained and imaged in parallel (2X*dpp*).

At stage 6, when the WT response domain narrows and nuclear Medea intensifies at the dorsal midline, all embryos from this mating had a narrow stripe of activated SMAD that covered a similar domain to WT (data not shown). Thus, neither *1Xdpp* nor *3Xdpp* altered the transition to a narrow midline response. However, the strength of the response was much lower in *1Xdpp* embryos by stage 7 (Fig. 7B). At the end of gastrulation, *3Xdpp* and *1Xdpp* embryos were easily distinguished (Fig. 7A-F). *3Xdpp* embryos had a broader midline response domain than WT, particularly in the cephalic region. 1X*dpp* embryos had narrower and weaker midline responses, as measured by either nuclear Medea (Fig. 5C, Fig. 7F) or PMAD (Fig. 7D). At stage 8, some 1X*dpp* embryos had a weak midline response (Fig. 7F); in others, it was undetectable (Fig. 7D). The variable midline response in

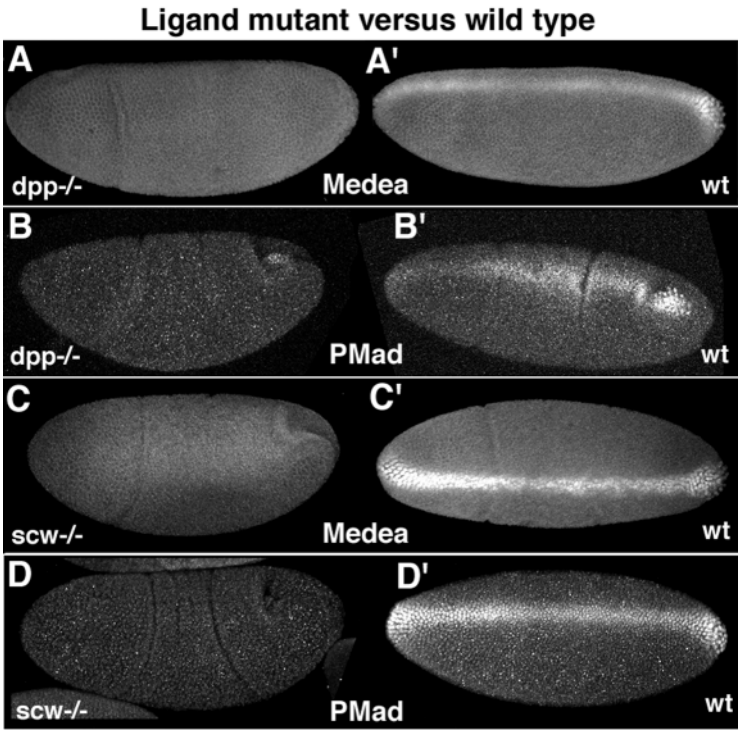

Fig. 6. Both BMP ligands are required for nuclear SMAD responses. Confocal projections of stage 6/7 embryos stained for Medea (A,A',C,C') or PMAD (B,B',D,D'), dorsolateral views except C',D' are dorsal. Mutants at left (A-D), with gain-matched wild-type (WT) controls at right (A'-D'). For each mutant-WT pair (e.g. A and A'), contrast was manipulated coordinately; contrast and confocal gain differ between different pairs. (A,B) In dpp^{H46} embryos, neither Medea nor PMAD is detectable in nuclei in any region. (C) In scw^{s12} embryos, Medea does not accumulate in nuclei, although apical staining is slightly more intense in approximately the dorsal 40% of the embryo. (D) PMAD levels are at background in somatic cells of scw^{s12} mutants. Anterior is leftwards.

1X*dpp* embryos fits the terminal phenotypes. All dpp^{H46}/+ embryos have defects in the head skeleton and head involution; reduced amnioserosa is less penetrant (Wharton et al., 1993).

In sum, the transition to a narrow dorsal midline response occurs normally with a 50% reduction in *dpp* gene dosage. Levels of DPP determine the width of the response domain and the level of peak response.

Increased Medea expands the amnioserosa

Levels of nuclear Medea in dorsal regions correlate well with the DV patterning outcome, supporting the model that nuclear SMAD activity is the functional output of BMP signaling. Studies of cultured cells indicate that increased SMAD protein levels can increase target gene expression (reviewed by Derynck et al., 1998). If the level of nuclear SMAD determines cell fate, then increased Medea levels should expand the most dorsal fate, the amnioserosa. We tested this with overexpressed Medea.

To assess the number of cells that acquire the amnioserosa fate, we counted Krüppel-positive amnioserosa nuclei in stage 13 embryos. Overexpression throughout development, in *ubi>Medea* embryos, gave 224±6 (average±s.e.m.; n=11) Krüppel-positive nuclei, significantly more than the WT 159±5 (n=10; P<0.01 by the two-tailed t test). *ubi>Medea* embryos also had subtly increased dorsal midline P-MAD staining (Fig.

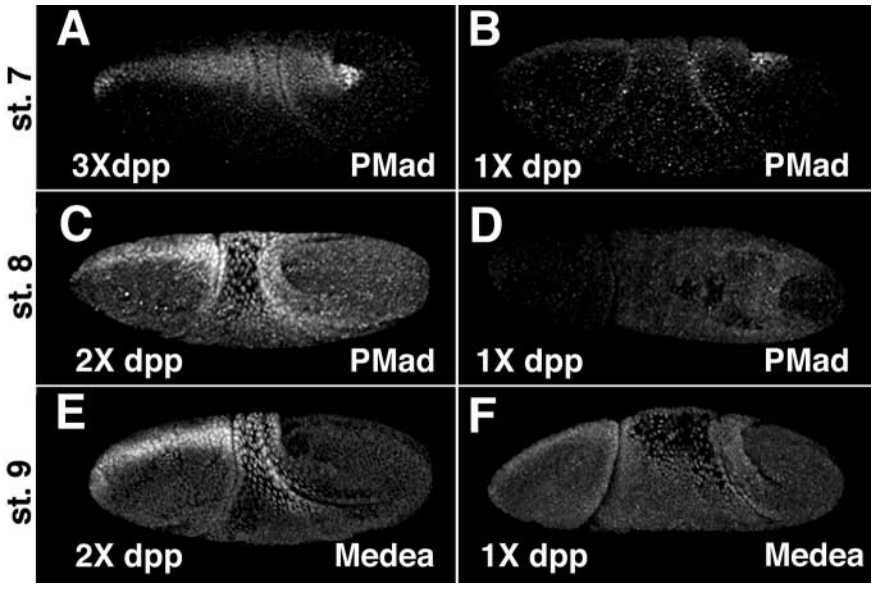

Fig. 7. The final level of SMAD response is sensitive to *dpp* gene dosage. Confocal projections of embryos stained for Medea (E,F) or PMAD (A-D). *2Xdpp* embryos are wild-type (WT) controls, *1Xdpp* and *3Xdpp* are dpp^{H46}/dpp^{+} and dpp^{+} $P\{dpp^{H+}\}/dpp^{+}$, respectively. (A) Stage 7, *3Xdpp* embryos show an expanded dorsal region of PMAD staining, which broadens in the trunk region as amnioserosa cells flatten. (B) Stage 7 *1Xdpp* embryos have weaker PMAD staining. Stage 8 *1Xdpp* embryos (D,F) have substantially weaker SMAD responses than WT. (D) Stage 8, 1Xdpp embryo with undetectable PMAD staining and partially ventralized phenotype. (E) In stage 9 WT has strong nuclear Medea accumulation in the amnioserosa and dorsal-midline of cephalic region. (F) Stage 9 *1Xdpp* embryos often have a weak stripe of nuclear Medea accumulation in the cephalic region and variable but low levels in amnioserosa nuclei.

5F). Thus, increased levels of co-SMAD can expand the domain of a BMP-induced cell fate. In an initial assessment of the critical period for this effect, we overexpressed Medea after gastrulation, in *prd>Gal4*; *UAS>Medea* embryos. Increased expression was detected at stage 9 (data not shown), but the number of amnioserosa cells was not significantly different from WT.

SOG shapes the SMAD response gradient

SOG has a complex role in DV patterning, for it both antagonizes dorsal ectoderm patterning and promotes the amnioserosa fate (Decotto and Ferguson, 2001). Patterns of SMAD responses should indicate whether the positive effect of SOG is transmitted through the BMP signaling pathway, but reports of PMAD patterns in *sog* mutants are conflicting (Dorfman and Shilo, 2001; Ross et al., 2001; Rushlow et al., 2001). To examine co-SMAD responses, we selected a strong allele, sog^{Y506}, and a molecular null, sog^{U2} (Francois et al., 1994). The two alleles gave similar results, assessed in stage 6 embryos.

For both Medea and PMAD staining, we detected three classes of embryos produced by heterozygous adults. One class appeared WT, and included the +/+ embryos (sog^{U2}: 19/43; sog^{Y506}: 3/16) (Fig. 8A,B). A second class showed an intense dorsal stripe of staining that was variably broader than WT (sog^{U2}: 19/43; sog^{Y506}: 10/16) (Fig. 8C,D), and probably included *sog*+/– females. The third class lacked the dorsal stripe of intense staining (sog^{U2}: 5/43; sog^{Y506}: 3/16) (Fig. 8E,F). These embryos had a broad dorsal domain with low levels of nuclear Medea (Fig. 8E) or weak PMAD staining (Fig. 8F), and were most probably *sog*–/–.

For both nuclear Medea and PMAD, reduced *sog* dosage was associated with a broader dorsal stripe, similar to that seen with increased *dpp* dosage (compare Fig. 8C,D with Fig. 5D and Fig. 7A). This mild *sog* dosage effect is consistent with effects on BMP target gene expression (Biehs et al., 1996). In the most extreme phenotype, the SMAD response domain covered almost half the circumference of the embryo (Fig. 8E,F). These changes in the patterns of SMAD activity are consistent with a role of SOG as a BMP antagonist. However, the embryos with the broadest dorsal domain of nuclear Medea had only weak SMAD responses (compare Fig. 8E,F with Fig. 8A,B). Throughout the dorsal regions of such embryos, most cells had low Medea staining distributed between the cytoplasm and nucleus. A few dorsal cells had predominantly nuclear localization of Medea (arrow, Fig. 8E), which may account for differentiated amnioserosa cells in null embryos (e.g. Jazwinska et al., 1999). A similar decrease was observed for PMAD staining (Fig. 8F). Response levels increased little during gastrulation (data not shown). Thus, SOG narrows the response domain and elevates the peak response.

Discussion

The roles of BMPs in dorsal patterning are well established, but the model for a simple spatial gradient of BMP activity is not supported by SMAD response data. Our data separate BMP activity into three phases, providing insight into the logic of patterning. Understanding the relationship between phases of BMP activity and patterning outcomes will be crucial for both testing molecular mechanisms and evaluating computational models for gradient formation.

BMP activity directs nuclear accumulation of co-SMAD in early embryos

These in vivo studies validate the molecular model for signal-dependent nuclear accumulation of co-SMAD. Nuclear accumulation of Medea requires both competence to oligomerize and an R-SMAD, MAD. Nuclear accumulation is signal dependent, requiring both BMP ligands, DPP and SCW. Conversely, all cells accumulated nuclear Medea in the presence of constitutively active TKV receptor. At these stages, any independent contribution from activin-like signals is below the detection limit.

Furthermore, levels of Medea determine the strength of BMP responses at these stages. Medea overexpression led to expansion of the dorsal-most fate, with increased numbers of amnioserosa cells. Signal-dependence for nuclear accumulation was retained (data not shown). Decreased Medea exacerbates loss of amnioserosa from reduced DPP levels (Raftery et al., 1995).

The intensity of Medea staining was surprisingly sensitive to signal activity. However, our tests showed that steady-state

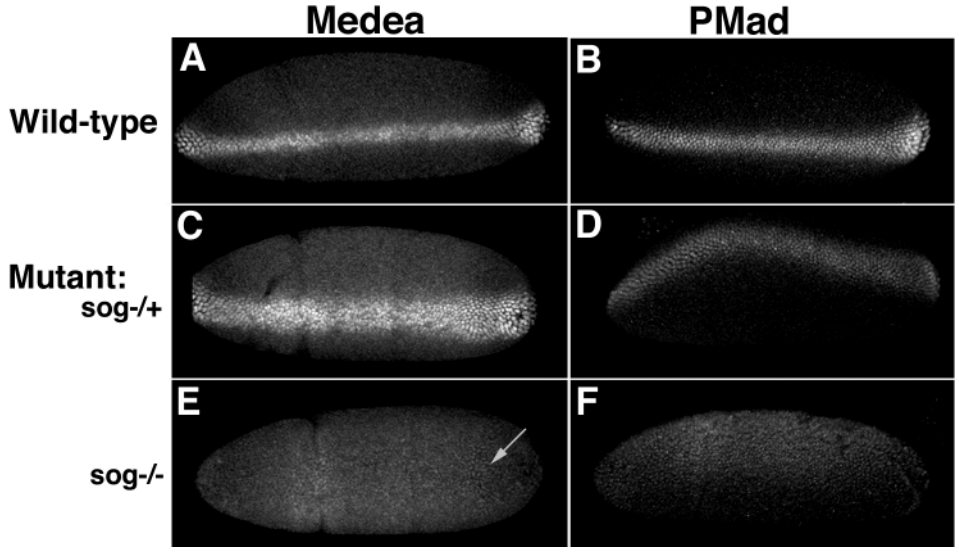

Fig. 8. SOG reduces the width and increases the level of SMAD response. Embryos from *sog* heterozygous parents stained for Medea (A,C,E) or PMAD (B,D,F), here shown for sog^{U2} (C-F) compared with wild type (A,B). (C,D) One aberrant class, inferred to be sog^{U2}/+, has a variably broader dorsal stripe of nuclear SMAD responses. (E,F) The other aberrant class, inferred to be sog^{U2} hemizygous males, has a low-level response over the dorsal half of the embryo. A region of cells with predominantly nuclear Medea is indicated (E, arrow). Anterior is leftwards.

levels of Medea were unaffected by the level of BMP activity. Our antibodies appeared highly sensitive to a Medea conformation that is prevalent in the nucleus, most probably an active SMAD complex. This sensitivity makes nuclear Medea an excellent assay to distinguish spatial patterns of endogenous BMP activity.

SMAD responses reveal dynamic patterns of BMP activity

In WT embryos, two transitions in the distribution of BMP activity were evident (Fig. 9). Many cellular blastoderm embryos lacked detectable levels of nuclear Medea, but a few had low levels of nuclear Medea in a broad dorsal domain, with little gradation (Fig. 9A). From the proportion of cellular blastoderm embryos with this pattern, it appears to be brief. These data parallel reports of broad, weak PMAD staining during mid-cellularization (Ross et al., 2001; Rushlow et al., 2001), except that nuclear Medea is detected later and in a broader pattern. The time lag between the earliest reported detection of PMAD and our detection of nuclear Medea probably stems from a combination of technical differences and the time necessary for nuclear accumulation. In sum, initial BMP activity is weak and distributed broadly in dorsal regions. Low BMP activity at this phase is required to maintain the early phase of *zen* expression (Rushlow et al., 2001).

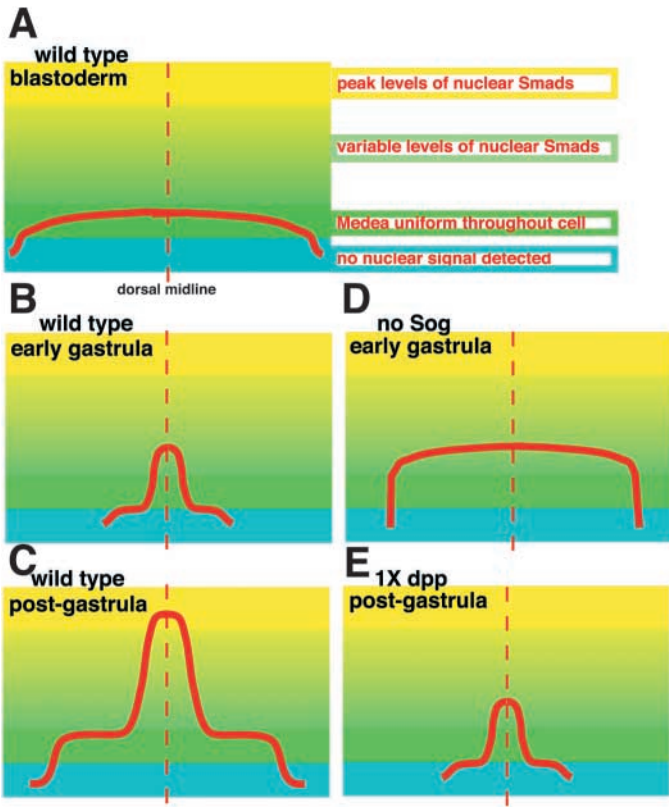

Fig. 9. Patterns of SMAD responses reveal stepwise changes in BMP activity. (A) When nuclear Medea was detected during stage 5, it was at uniformly low levels across about 24 dorsal nuclei, and then declined across four nuclei at each edge. (B) At the beginning of stage 6, a narrow stripe of more intense nuclear Medea staining was detected at the dorsal midline. Nuclear Medea was no longer detected in dorsolateral regions, even though staining levels rose at the dorsal midline. (C) Levels of nuclear Medea peaked in dorsal midline cells during stage 7, and adjacent domains of low nuclear Medea became detectable on either side. At this stage, the entire nuclear Medea response domain was not as wide as the initial response domain during stage 5. (D) Stage 6 *sog* hemizygous embryos (no Sog) had a broad domain with low levels of nuclear Medea and PMAD. Levels were higher than wild-type stage 5 embryos, but did not reach the peak levels seen in wild type. (E) Heterozygous *dpp* embryos (1X dpp) formed a narrow dorsal midline stripe, but the levels of nuclear Medea and PMAD did not reach the peak levels seen in wild type. During stages 7 and 8, a narrower stripe was sometimes evident in the cephalic region of these embryos.

Onset of gastrulation was associated with a dramatic change in the domain of nuclear Medea, which narrowed to a tight midline stripe of cells while staining levels intensified (Fig. 9B). PMAD shows a similar transition to a narrower domain, but earlier (Ross et al., 2001; Rushlow et al., 2001). Thus, lateral SMAD responses became undetectable just as a steep activity gradient formed along the dorsal midline.

A third response pattern arose during mid-gastrulation; dorsolateral domains of cells exhibited low levels of nuclear Medea (Fig. 9C). Response levels remained high in the dorsal-most cells, even as they moved laterally during gastrulation (Fig. 3E, Fig. 4A). Levels fell off rapidly over a few cells on either side, with a sharp transition to flanking plateaus of weak responses. The subcellular distribution of Medea was unchanging in ventral and ventrolateral cells. The full BMP response domain did not extend as far ventrally as it did during blastoderm, even though many dorsal cells move laterally during germband extension (Campos-Ortega and Hartenstein, 1997). Thus, the lateral-most cells with responses at blastoderm had decreased responses during gastrulation.

In sum, the dorsal midline stripe of SMAD responses corresponds to a steep BMP activity gradient, with thresholds that correlate with patterning markers. The edges of the Medea peak response correlated precisely with the position of dorsal cephalic markers during stage 8, the cycle 14 mitotic domains 1, 3 and 5. The second phase of *zen* expression occurs in cells with peak PMAD responses at the end of stage 5 (Rushlow et al., 2001). Flanking cells with lower PMAD levels correlate with the broader expression domain for the BMP target genes *tailup* and *u-shaped* (Ashe et al., 2000; Rushlow et al., 2001). The full Medea response domain correlates approximately with the expression domain for *u-shaped* and extends into the presumptive dorsomedial ectoderm. The sharp transitions in SMAD response levels predict expression boundaries for BMP-responsive genes.

Similarly, in the wing primordium, a BMP gradient creates sharp transitions in PMAD levels, which match gene expression boundaries (Tanimoto et al., 2000; Teleman and Cohen, 2000). However, BMP activity is modulated by different mechanisms in this tissue. *dpp* is expressed in a narrow stripe at the center, and ligand spreads to nearby cells over a period of hours. In contrast, the early embryonic BMP activity gradient forms rapidly, and is narrower than the expression domains for *dpp* and *scw*. Extracellular binding proteins form the embryonic BMP activity gradient.

The dorsal midline gradient is shaped by DPP and SOG

The final width of the midline peak response is sensitive to

gene dosage for both *dpp* and *sog*. It is broader when *dpp* dosage is increased (Fig. 5D, Fig. 7A), and narrower with only one copy of *dpp* (Fig. 5C, Fig. 7F, Fig. 9E). Similarly, the width of the stripe was broader, but more variable, when *sog* levels were reduced (Fig. 8C,D, Fig. 9D). The response domain was broadest in *sog* null embryos (Fig. 8E,F); however, the level of response was significantly reduced. This was distinct from the effect of increased *dpp* dosage, in which the response domain was broader, but normal SMAD response levels were achieved or exceeded.

The role of SOG as both a short-range inhibitor and a long-range potentiator of dorsal patterning led to a proposal that SOG transports BMP ligands from lateral regions to the dorsal midline (Holley et al., 1996). Biochemical analyses suggest mechanisms for SOG-BMP binding and release (reviewed by Harland, 2001; Ray and Wharton, 2001). Computational analysis defined conditions under which transport could occur with these mechanisms (Eldar et al., 2002). The transition from weak, broad SMAD responses to narrow, strong responses is consistent with concentration of BMP activity at the dorsal midline, and the loss of this transition with loss of SOG is consistent with a SOG-dependent transport model. However, there are significant differences between our results and the assumptions used to develop the computational model. These include the presence of a midline SMAD response in *dpp*–/+ embryos and the sensitivity to reduced *sog* dosage. It will be important to refine future computational models to fit the complete set of BMP response data.

Altered activity at different phases affects different tissue boundaries

Both BMP ligands, DPP and SCW, were required to form the dorsal-midline gradient. However, *scw* mutant embryos retain a small amount of dorsal ectoderm, with concomitant expansion of ventral ectoderm (Arora et al., 1994). Surprisingly, the weak dorsolateral Medea response is lost in *scw* embryos. We conclude that the full Medea response domain encompasses the cell fates that are lost in *scw* mutants, amnioserosa and dorsomedial ectoderm (Arora and Nüsslein-Volhard, 1992). It appears that dorsal cells can acquire a dorsolateral fate without gastrula BMP activity.

Mutants with expanded ventral ectoderm show reduced SMAD responses during the first phase of BMP activity. PMAD was not detected in blastoderm *tld* embryos (Ross et al., 2001). Homozygotes for moderate *dpp* alleles have lower PMAD levels during blastoderm (Rushlow et al., 2001). Conversely, *sog* embryos have a slightly expanded PMAD response during blastoderm (Rushlow et al., 2001), and a slight expansion of dorsal ectoderm (Ferguson and Anderson, 1992b). Thus, BMP activity during blastoderm positions the boundary between dorsal and ventral ectoderm.

Mutations that shift the boundary between amnioserosa and dorsal ectoderm show altered SMAD responses in the third phase of BMP activity, the dorsal-midline gradient. *dpp*–/+ embryos had variable reductions in midline SMAD responses (Fig. 7) and in the number of amnioserosa cells (Wharton et al., 1993). Strikingly, *sog* null embryos have little amnioserosa and a strong reduction in SMAD response levels during gastrulation (Fig. 8). Thus, SMAD response levels during gastrulation are critical for amnioserosa specification.

Multiple rounds of BMP signaling pattern DV fates

Taken together, these data suggest a multi-step model for DV patterning of the embryonic ectoderm, incorporating aspects of the two previous models. In the previous gradient model, ectodermal fates are subdivided simultaneously by a continuous BMP gradient involving DPP and SCW (Ferguson and Anderson, 1992a). In the successive cell-fate decision model, amnioserosa is specified by dorsal-midline DPP+SCW activity, and the dorsal ectoderm by DPP alone at stage 9 (Dorfman and Shilo, 2001).

Instead, we propose that the blastoderm phase of weak BMP activity establishes a dorsal ectoderm domain. As discussed above, mutations that shift the boundary between dorsal and ventral ectoderm also have altered SMAD responses at this stage. It is at this stage that SMADs compete with Brinker to regulate the first phase of *zen* expression (Rushlow et al., 2001). Furthermore, this early signal maintains BMP activity, for the late-blastoderm domain of *dpp* expression is set by competition between BMPs, SOG and Brinker (Biehs et al., 1996; Jazwinska et al., 1999). BMP activity subsequently maintains the dorsal boundary for *brinker* expression (Jazwinska et al., 1999). Thus, BMP activity at blastoderm defines a dorsal domain where *dpp* is expressed and *brinker* is not.

After cellularization is complete, a step gradient of BMP activity subdivides the dorsal region into amnioserosa, dorsomedial ectoderm and dorsolateral ectoderm. Peak activity levels determine the amount of amnioserosa. Flanking shoulders of weak activity specify the dorsomedial ectoderm. We propose that the dorsolateral ectoderm experiences a transient BMP response during late blastoderm, but little or no response during gastrulation. In sum, the dorsal-midline gradient of BMP activity specifies at least three cell fates.

BMP activity in the dorsal ectoderm does not end with germband extension. During stage 9, PMAD is detected throughout the dorsal ectoderm and amnioserosa, and might finalize determination of dorsal ectoderm fates (Dorfman and Shilo, 2001). DPP expression within the dorsal ectoderm contributes to combinatoral regulation of gene expression patterns in subsets of dorsal ectodermal cells (Reim et al., 2003). However, the ventral boundary of *dpp* expression in the stage 9 dorsal ectoderm must be defined by earlier events.

Implications for molecular mechanisms

The step gradient of SMAD responses is maintained during the morphogenetic movements of gastrulation and germband extension. The peak response is maintained only in cells that initially resided at the dorsal midline, even though ventral ectoderm moves to a dorsal position during stages 7 and 8. The BMP activity gradient is thought to form by diffusion in the perivitelline fluid; however, dorsal cells ‘remember’ their BMP exposure as they move laterally [perhaps similar to memory of signal strength as discussed in Bourillot et al. (Bourillot et al., 2002)]. It is probable that the ligand distribution is established prior to the time that peak SMAD responses are detected, and activity persists through cell biological mechanisms. For example, ligand may bind to the extracellular matrix (Fujise et al., 2003), so that it remains associated with dorsal cells. Alternatively, receptor-ligand complexes may continue to signal following endocytosis, as described for TGFβ (Penheiter et al., 2002). Understanding the intracellular modulation of

BMP responses will be important to understand how extracellular morphogen gradients are translated into a stable pattern of cell fates.

We thank P. ten Dyke for anti-phospho-SMAD1; M. Cutler, A. Jaeger, J. Monterecy and M. Pazin for technical support; M. O'Connor, B. Morgan and J. Gurdon for discussions; T. Tabata and B. Shilo for sharing data; K. Barrett, C. Ferguson, R. Padgett, M. O'Connor and the Bloomington Stock Center for flies. This work was supported by grants from the American Cancer Society (DB-147) and the NIH (GM60501).

References

Arora, K., Levine, M. S. and O'Connor, M. B. (1994). The *screw* gene encodes a ubiquitously expressed member of the TGF-β family required for specification of dorsal cell in the *Drosophila* embryo. *Genes Dev.* **8**, 2588-2601.

Arora, K. and Nüsslein-Volhard, C. (1992). Altered mitotic domains reveal fate map changes in *Drosophila* embryos mutant for zygotic dorsoventral patterning genes. *Development* **114**, 1003-1024.

Ashe, H. L. and Levine, M. (1999). Local inhibition and long-range enhancement of Dpp signal transduction by Sog. *Nature* **398**, 427-431.

Ashe, H. L., Mannervik, M. and Levine, M. (2000). Dpp signaling thresholds in the dorsal ectoderm of the *Drosophila* embryo. *Development* **127**, 3305-3312.

Barrett, K., Leptin, M. and Settleman, J. (1997). The Rho GTPase and a putative RhoGEF mediate a signaling pathway for the cell shape changes in *Drosophila* gastrulation. *Cell* **81**, 905-915.

Biehs, B., François, V. and Bier, E. (1996). The *Drosophila short gastrulation* gene prevents Dpp from autoactivating and suppressing neurogenesis in the neuroectoderm. *Genes Dev.* **10**, 2922-2934.

Bourillot, P. Y., Garrett, N. and Gurdon, J. B. (2002). A changing morphogen gradient is interpreted by continuous transduction flow. *Development* **129**, 2167-2180.

Brand, A. H. and Perrimon, N. (1993). Targeted gene expression as a means of altering cell fates and generating dominant phenotypes. *Development* **118**, 401-415.

Campos-Ortega, J. and Hartenstein, V. (1997). *The Embryonic Development of* Drosophila melanogaster. Berlin, Germany: Springer-Verlag.

Campos-Ortega, J. A. and Hartenstein, V. (1985). *The Embryonic Development of* Drosophila melanogaster. Berlin, Germany: Springer-Verlag.

Chou, T. and Perrimon, N. (1996). The autosomal FLP-DFS technique for generating germline mosaics in *Drosophila melanogaster*. *Genetics* **144**, 1673-1679.

Das, P., Maduzia, L., Wang, H., Finelli, A., Cho, S., Smith, M. and Padgett, R. (1998). The *Drosophila* gene *Medea* demonstrates the requirement for different classes of Smads in *dpp* signaling. *Development* **125**, 1519-1528.

Decotto, E. and Ferguson, E. L. (2001). A positive role for Short gastrulation in modulating BMP signaling during dorsoventral patterning in the *Drosophila* embryo. *Development* **128**, 3831-3841.

Derynck, R., Zhang, Y. and Feng, X. H. (1998). Smads: transcriptional activators of TGF-β responses. *Cell* **95**, 737-740.

Dobens, L. L., Peterson, J., Treisman, J. and Raftery, L. A. (2000). *Drosophila bunched* integrates opposing DPP and EGF signals to set the operculum boundary. *Development* **127**, 745-754.

Dorfman, R. and Shilo, B. Z. (2001). Biphasic activation of the BMP pathway patterns the *Drosophila* embryonic dorsal region. *Development* **128**, 965-972.

Eldar, A., Dorfman, R., Weiss, D., Ashe, H., Shilo, B. Z. and Barkai, N. (2002). Robustness of the BMP morphogen gradient in *Drosophila* embryonic patterning. *Nature* **419**, 304-308.

Ferguson, E. L. and Anderson, K. V. (1992a). *decapentaplegic* acts as a morphogen to organize dorsal-ventral pattern in the *Drosophila* embryo. *Cell* **71**, 451-461.

Ferguson, E. L. and Anderson, K. V. (1992b). Localized enhancement and repression of the activity of the TGF-β family member, *decapentaplegic*, is necessary for dorsal-ventral pattern formation in the *Drosophila* embryo. *Development* **114**, 583-597.

Foe, V. E., Odell, G. M. and Edgar, B. A. (1993). Mitosis and morphogenesis in the *Drosophila* embryo: point and counterpoint. In *The Development of* Drosophila melanogaster (ed. M. Bate and A. Martinez-Arias), pp. 149-300. Plainview, NY: Cold Spring Harbor Laboratory Press.

Francois, V., Solloway, M., O'Neill, J. W., Emery, J. and Bier, E. (1994). Dorsal-ventral patterning of the *Drosophila* embryo depends on a putative negative growth factor encoded by the *short gastrulation* gene. *Genes Dev.* **8**, 2602-2616.

Fujise, M., Takeo, S., Kamimura, K., Matsuo, T., Aigaki, T., Izumi, S. and Nakato, H. (2003). Dally regulates Dpp morphogen gradient formation in the *Drosophila* wing. *Development* **130**, 1515-1522.

Gurdon, J. B. and Bourillot, P. Y. (2001). Morphogen gradient interpretation. *Nature* **413**, 797-803.

Haerry, T., Khalsa, O., O'Connor, M. and Wharton, K. (1998). Synergistic signaling by two BMP ligands through the SAX and TKV receptors controls wing growth and patterning in *Drosophila*. *Development* **125**, 3977-3987.

Harland, R. M. (2001). Developmental biology. A twist on embryonic signalling. *Nature* **410**, 423-424.

Harlow, E. and Lane, D. (1988). *Antibodies: A Laboratory Manual*. Cold Spring Harbor, NY: Cold Spring Harbor Laboratory Press.

Holley, S. A., Neul, J. L., Attisano, L., Wrana, J. L., Sasai, Y., O'Connor, M. B., De Robertis, E. M. and Ferguson, E. L. (1996). The *Xenopus* dorsalizing factor noggin ventralizes *Drosophila* embryos by preventing DPP from activating its receptor. *Cell* **86**, 607-617.

Hudson, J., Podos, S., Keith, K., Simpson, S. and Ferguson, E. (1998). The *Drosophila Medea* gene is required downstream of *dpp* and encodes a functional homolog of human Smad4. *Development* **125**, 1407-1420.

Irish, V. F. and Gelbart, W. M. (1987). The *decapentaplegic* gene is required for dorsal/ventral patterning of the *Drosophila* embryo. *Genes Dev.* **1**, 868-879.

Jazwinska, A., Rushlow, C. and Roth, S. (1999). The role of *brinker* in mediating the graded response to Dpp in early *Drosophila* embryos. *Development* **126**, 3323-3334.

Li, M., Strand, D., Krehan, A., Pyerin, W., Heid, H., Neumann, B. and Mechler, B. M. (1999). Casein kinase 2 binds and phosphorylates the nucleosome assembly protein-1 (NAP1) in *Drosophila melanogaster*. *J. Mol. Biol.* **293**, 1067-1084.

Massague, J. and Wotton, D. (2000). Transcriptional control by the TGF-beta/Smad signaling system. *EMBO J.* **19**, 1745-1754.

Neul, J. and Ferguson, E. (1998). Spatially-restricted activation of the SAX receptor by SCW modulates DPP/TKV signaling in *Drosophila* dorsal/ventral patterning. *Cell* **95**, 483-494.

Neumann, C. and Cohen, S. (1997). Morphogens and pattern formation. *BioEssays* **19**, 721-729.

Newfeld, S. J., Mehra, A., Singer, M. A., Wrana, J. L., Attisano, L. and Gelbart, W. M. (1997). *Mothers against dpp* participates in a DPP/TGF-β responsive serine-threonine kinase signal transduction cascade. *Development* **124**, 3167-3176.

Nguyen, M., Park, S., Marqués, G. and Arora, K. (1998). Interpretation of a BMP activity gradient in *Drosophila* embryos depends on synergistic signaling by two type I receptors SAX and TKV. *Cell* **95**, 495-506.

Penheiter, S. G., Mitchell, H., Garamszegi, N., Edens, M., Dore, J. J., Jr and Leof, E. B. (2002). Internalization-dependent and -independent requirements for transforming growth factor beta receptor signaling via the Smad pathway. *Mol. Cell Biol.* **22**, 4750-4759.

Persson, U., Izumi, H., Souchelnytskyi, S., Itoh, S., Grimsby, S., Engstrom, U., Heldin, C. H., Funa, K. and ten Dijke, P. (1998). The L45 loop in type I receptors for TGF-beta family members is a critical determinant in specifying Smad isoform activation. *FEBS Lett.* **434**, 83-87.

Pierreux, C. E., Nicolas, F. J. and Hill, C. S. (2000). Transforming growth factor beta-independent shuttling of Smad4 between the cytoplasm and nucleus. *Mol. Cell Biol.* **20**, 9041-9054.

Podos, S. D. and Ferguson, E. L. (1999). Morphogen gradients: new insights from DPP. *Trends Genet.* **15**, 396-402.

Raftery, L. and Sutherland, D. (1999). TGF-β family signal transduction in *Drosophila*: from *Mad* to Smads. *Dev. Biol.* **210**, 251-268.

Raftery, L. A., Twombly, V., Wharton, K. and Gelbart, W. M. (1995). Genetic screens to identify elements of the *decapentaplegic* signaling pathway in *Drosophila*. *Genetics* **139**, 241-254.

Ray, R. P. and Wharton, K. A. (2001). Twisted perspective: new insights into extracellular modulation of BMP signaling during development. *Cell* **104**, 801-804.

Reim, I., Lee, H.-H. and Frasch, M. (2003). The T-box-encoding *dorsocross* genes function in amnioserosa development and the patterning of the dorsolateral germ band downstream of Dpp. *Development* **130**, 3187-3204.

Ross, J. J., Shimmi, O., Vilmos, P., Petryk, A., Kim, H., Gaudenz, K., Hermanson, S., Ekker, S. C., O'Connor, M. B. and Marsh, J. L. (2001). Twisted gastrulation is a conserved extracellular BMP antagonist. *Nature* **410**, 479-483.

Roth, S., Hiromi, Y., Godt, D. and Nusslein-Volhard, C. (1991). *cactus*, a maternal gene required for proper formation of the dorsoventral morphogen gradient in *Drosophila* embryos. *Development* **112**, 371-388.

Rushlow, C., Colosimo, P. F., Lin, M., Xu, M. and Kirov, N. (2001). Transcriptional regulation of the *Drosophila* gene *zen* by competing Smad and Brinker inputs. *Genes Dev.* **15**, 340-351.

Slack, J. (1991). *From Egg to Embryo: Regional Specification in Early Development*. Cambridge, UK: Cambridge University Press.

Srinivasan, S., Rashka, K. E. and Bier, E. (2002). Creation of a Sog morphogen gradient in the *Drosophila* embryo. *Dev. Cell* **2**, 91-101.

St. Johnston, R. D. and Gelbart, W. M. (1987). *decapentaplegic* transcripts are localized along the dorsal-ventral axis of the *Drosophila* embryo. *EMBO J.* **6**, 2785-2791.

Tanimoto, H., Itoh, S., ten Dijke, P. and Tabata, T. (2000). Hedgehog creates a gradient of DPP activity in *Drosophila* wing discs. *Mol. Cell* **5**, 59-71.

Teleman, A. A. and Cohen, S. M. (2000). Dpp gradient formation in the *Drosophila* wing imaginal disc. *Cell* **103**, 971-980.

Wharton, K. A., Ray, R. and Gelbart, W. M. (1993). An activity gradient of *decapentaplegic* is required for dorsal-ventral patterning in the *Drosophila* embryo. *Development* **117**, 807-822.

Wisotzkey, R. G., Mehra, A., Sutherland, D., Dobens, L. L., Dohrmann, C., Attisano, L. and Raftery, L. A. (1998). *Medea* is a *Drosophila Smad4* homolog that is differentially required to potentiate DPP responses. *Development* **125**, 1433-1445.

Xu, X., Yin, Z., Hudson, J., Ferguson, E. and Frasch, M. (1998). Smad proteins act in combination with synergistic and antagonistic regulators to target Dpp responses to the *Drosophila* mesoderm. *Genes Dev.* **12**, 2354-2370.

Zhang, H., Levine, M. and Ashe, H. L. (2001). Brinker is a sequence-specific transcriptional repressor in the *Drosophila* embryo. *Genes Dev.* **15**, 261-266.